Multi-angle Imaging SpectroRadiometer (MISR):

Optical Characterization of the Spectralon Calibration Panels

B.T. McGuckin, D.A. Haner and R.T. Menzies

Jet Propulsion Laboratory

California Institute of Technology

4800 Oak Grove Drive

Pasadena CA 91109

Abstract

The reflectance properties of an engineering model of the Spectral on panel intended for use within an On Board Calibrator (OBC) on the NASA Multi-angle Imaging SpectroRadiometer (MISR) instrument have been fully characterized with regard to panel uniformity and isotropy in response to three incident laser wavelengths of 442, 632.8 and 859.9 nm. A regional variation in bidirectional reflectance function (BRF) across the surface of the engineering model (EM) panel, contributing to spatial non-uniformity at the ± 2% level has been measured at all three laser wavelengths. Further, a BRF anisotropy has been identified. The mechanism causing these departures from the ideal Lambertian surface may originate in the sanding of the SpectraIon surface in the final stage of preparation. This is corroborated by measurements made on a "pressed" polytetrafluoroethylene (PTFE) panel in which a greatly reduced anisotropy in panel BRF is measured. The EM panel BRF reveals deviation from a Lambertian characteristic manifest as an off-specular peak in the forward

scattering direction. A common cross-over point at an angle of reflection of around 370 at which the BRF is constant within+ 0.4% for an illumination angle range of θ, = 30°- 60° is observed at all three wavelengths.

Two SpectraIon protoflight panels which were fabricated after the engineering model was studied were also the subject of a uniformity study over part of the area of the SpectraIon panels at the 442 nm wavelength. The analysis indicated that the panel uniformity satisfies the ± O. 5°/0 criterion indicating improved panel preparation. However, the off specular peak in the forward scattering direction is essentially unchanged with the cross-over point at approximately 37°.

1. Introduction

The Multi-angle Imaging SpectroRadiometer (MISR) is presently being designed and built at the Jet Propulsion Laboratory as an Earth Observing System (EOS) flight instrument due for launch in 1998. MISR will obtain global multi-angle, radiometrically calibrated imagery from a suite of nine cameras pointed toward the earth each at a unique angle and at four spectral bands per camera. Optical properties of tropospheric aerosols, the bidirectional reflectance distribution function of the earth surface and clouds, together with cloud heights, wi 11 be deduced, These data will be used in conjunction with other data from multi spectral imaging to enhance the understanding of the many and varied natural and anthropogenic processes which modify the climate and ecology of the Earth(').

In order to meet the requirement that an absolute radiometric calibration be maintained to within ±3% uncertainty throughout the five year mission life, a key part of the instrument is an On-Board Calibrator (OK) sub-system. Integral to the OBC are a pair diffuse panels which will be deployed at approximately monthly intervals over the poles to reflect solar irradiance into the cameras for in-flight calibration. When not in use the panels wil I be stowed and protected '2).

The panels are used to provide a uniform, "flat-field" scene while radiance scaling is achieved with use of OBC photodiode standards. To facilitate pixel to pixel calibration of the CCD cameras, the panel reflected radiance must bc highly uniform over the whole usable surface. Further, Lambertian performance would simplify "camera to camera" calibrations. The manner in which the nine cameras arc mounted around the 51 cm long panel y-axis i reposes a stringent requirement of panel

spatial uniformity at the O. 5°/0 level over 2.5 cm intervals. SpectraIon was identified as the only commercially available material potentially capable of satisfying these demands and has therefore featured in a comprehensive series of pre-flight tests of the material's optical reflectance characteristics,

'l'he SpectraIon panels are fabricated with three positioning "cleats" to aid with the proper location of the panel into the aluminum tray during the life of the i nstrument. These cleats are small regions where the SpectraIon panel is 1.27 cm thick compared to the general panel thickness of 0.635 cm. In view of the volumetric nature of light scattering from Spectralon, it is an additional and an important objective to evaluate any influence "which these cleats may have on the 13 RF.

It "is the purpose of this paper to report on these tests with emphasis on the subset which have the specific objective of experimental] y quantifying the SpectraIon spatial uniformity. This uniformity is quantified through the measurement of the bidirectional reflectance factor '[3](B RF) of the panel at eleven spatially distinct locations repeated over a prescribed series of incidence and reflected angles.

2. BRF Test Setup

The detailed description of the calibration facility can be found in a previous publication '4); however a schematic of the optical layout used during this study is illustrated in Figure (1). The Spectralon panel is to bc characterized at three wavelengths chosen to be close to three of the four MISR

spectral bands centered at 443, 555, 670 and 865 nm. The three wavelengths chosen are all derived from laser sources respectively and are a helium cadmium (HeCd) lasing at 442 nm, a helium neon (HeNe) laser at 632.8 nm and a GaAIAs semiconductor diode laser source at 859.9 nm.

The relative amplitude of the light incident on the SpectraIon panel and the reference detector are controlled by a zero order half waveplate and polarizer combination with the latter oriented to pass p-polarized light (with a 500:1 extinction ratio) relative to the plane containing the detector and the incident beam, termed the principal plane. Scattered light from the panel is measured in both "s" and "p''-polarizations. Ratioing of the light scattered from the panel with that of the reference derived from a detector viewing the rejected light from the polarizer is employed to minimize signal noise due to amplitude fluctuations in the sources.

The detector channels are optically and electronically identical; both using 1 cm square silicon photodiodes with a noise equivalent power (NEP) of 1.8 x 1()-14 $W.Hz^{-1/2}$. The nearly identical sensitivity of the detectors over all three wavelength bands avoids unnecessary disturbance to the experiment when transitioning between wavelengths.

Each detector is housed in a telescope assembly built specifically for this task, and each detection channel uses phase sensitive detection and amplification and is interfaced to a PC computer for data acquisition and processing. The lock-in voltage signals are digitized by an A/D board occupying a 16-bit expansion slot in a 386 IBM compatible personal computer. The board has a 12-bit digitizer with a minimum sampling interval of-5 μs. The lock-in amplifier post-detection time constant and

the digitizer sampling interval input to the software menu are carefully selected to ensure that calculated and displayed standard deviation for each detection channel (and ratio) give a true representation of the system noise and provide adequate filtering.

The detector viewing the light scattered from the panel is mounted on a 30 cm long boom extending from the common axis of rotation of the panel and detector. All internal surfaces of both assemblies are painted matte black to minimize scattered light. The detector - panel separation and a 1 cm aperture stop establishes the detector resolution at $\leq 2°$. The boom is fabricated from slightly modified aluminum channel for increased mechanical stability. As a test of the mechanical stability, measurements reveal that the detector remains in the principal plane to a tolerance of 0.010 through a boom rotation of 180°.

An area of the panel of 2.54 cm diameter is imaged by the detector which, together with the field of view (FOV), are defined by the field stop (diameter = 0.56 cm) and the distance of the field stop from the relay lens (f = 6.29 cm). The detector oversamples the illuminated area on the panel, however, the imaged area is kept as close as practicable to the actual illuminated area in order to minimize the amount of incident and reflected stray light imaged onto the detector.

A spatial filter (SF) / beam expander combination is used to condition each beam to be 1.27 cm diameter at the panel at normal incidence in order to satisfy the detector spatial averaging requirement of one inch actual physical diameter when the angle of incidence $\theta_i = 60°$ and to reduce the spatial noise on the beam. The collimated beam from the diode laser at 859.9 nm is

approximately circular, measuring 8 mm across, 'I'his is large compared to the aperture of the input lens to the SF which leads to poor throughput and consequently, a different beam expander is used for 859.9 nm.

The Spectralon panel initially examined is an "Engineering Model" (EM) version of the material which will fly with the MISR instrument. The panel measures 57 x 6.35 x 0.635 cm and is contained within an aluminum tray. The tray is mounted in a computer controlled target assembly: rotary stages control the detector and target rotation. A goniometric cradle is used to position the target surface normal in and out of the principal plane. The cradle is capable of ± 45° travel and 0.010 resolution. Two adapters have been specifically fabricated which allow the target to be mounted to attain ± 90° tilt in and out of the principal plane. All stages have high torque dc motors and precision incremental encoders permitting control of target and detector position when interfaced to a computer. Both target and detector are capable of 360° rotation with 0.0010 resolution in the horizontal plane. Bi-directional repeatability is ().003°, accuracy 0.05° and backlash <0.05°. The precision of the mounting system was verified by measuring the movement of the surface normal out of principal plane to be $< \pm$ 0.06° over target rotation of ± 60°.

3. Measurement Methodology

The Spectralon BRF is measured at the three wavelengths at each of three angles of incidence of θ_i = 30, 45 and 600 and for $O < \theta_r < 70$ ° (in the principal plane) in 5 ° increments as shown in Figure 2. To reveal panel spatial uniformity, each run is repeated at eleven spatially distinct

positions on the panel surface illustrated in Figure 3. The location of each position is chosen to provide the widest possible coverage of the panel. Positions 5, 6 and 7 were selected in order to reveal any effect which the central cleat (located under position 6) may have on the reflectance - and by inference any effect by the cleats toward the two ends. The left and right cleats are not illuminated by the incident beam even when the area of the panel covered by the incident light is greatest i.e. when $\theta_i = 60°$.

Reference marks on the rear of the aluminum tray are used to orientate the particular numbered spot into the path of the incident laser beam. Initially measurements are made at positions 5, 6 and 7. To access positions 8 through 11 on the lower section of the panel, it is necessary to remove the panel and insert a spacer plate under the lower edge in to raise the panel by 15 mm. The panel is remounted and the reference marks again used to slide the desired area of the panel into the beam, Positions 1 through 4 also require use of the spacer plate and removal of the panel which must then be rotated through 180° to allow beam access to the panel location of interest. A consequence of this last step is that in comparing the data sets, only those obtained at positions 5 through 11 are consistent, i.e. the panel is mounted with the same orientation. For positions 1 through 4, while consistent in themselves, they should not be compared with those from other positions since 180° rotation about the panel normal is equivalent to viewing, the panel at $\phi_i + \pi$.

For each measurement of the eleven positions on the panel surface and at each wavelength, a unique data file is created as shown in Table 1. In the table, detector position is the location of the detector which is viewing the light scattered from the panel with the angles measured from the surface

normal (i.e. $\theta_r = 00$, for increasing θ_r in the forward scattering, direction. Channel O is the signal from the detector viewing the light scattered off the panel. The standard deviation calculated for a defined number of samples (usually 103) at each detector position. Channel 1 is a reference channel and is proportional to the incident light level, Channel O and Channel 1 voltages are ratioed and displayed as mean ratio along with the respective standard deviation,

Reflectance measurement repeatability on a run -to - run basis is measured to be < 0.2%. This test was extended to check repeatability after total e] ectrical shut-down, disassembly of the target and the elapse of several days between runs. In this instance repeatability was measured to be < 0.4°/0.

4. Spectralon BRF Spatial Uniformity

The panel uniformity is assessed by calculating the difference, %D, between the average value , X (0,), of the mean ratio column for all eleven panel positions and the mean ratio column, R(θ_r)for each panel position. This calculation is performed for each view angle, O $\leq \theta_r \leq 70°$; and defined by

$$X(\theta_r) = \frac{\sum_{1}^{11} R\ (0,)}{1\ \ 1} \quad \textit{for fixed } (\lambda,\theta_i)$$

and therefore,

$$\%D \cdot \frac{[R(\theta_r) - X(\theta_r)]}{X(\theta_r)} \ X\ 100$$

The EM panel uniformity is gauged by the spread in the value of %D as a function of view angle for each wavelength and angle of incidence. The value of %D as a function of θ_r is plotted in Figures 4, 5 and 6 for the specific case of $\theta_i = 600$ where the spread is greatest and any trends are more discernible. Each plot consists of eleven different traces corresponding to the difference between the BRF measured at each panel position and the average of the panel taken as a whole - shown as °/01) ⁼ O .

It is especially clear from Figure 4 that at 442 nm there are three disparate BRFs measurable from three distinct regions of the panel: One in which a group of four traces (panel positions 1 -4) follows a negative gradient from +2% above average down to average at $\theta_r = 70°$. A second group of four (from positions 8- 11) follows a positive slope in which the BRF increases from around the panel average to + 2°/0 and, finally, a third set of three traces in which the BRF measured from three positions (5, 6 and 7) are consistently 2- 3% below the panel average (with a slight downwards trend) over the range of θ_r.

In Figure 5 a similar pattern of response is evident (but slightly less pronounced) at 632.8 nm. The trends are even less discernible at 859.9 nm as shown in Figure 6. However, the 859.9 nm data were not prepared using the ratio to reference, but using only the reflectance detector signals directly, which increases the experimental noise.

The maximum and minimum values of %D when sampled over all spatial positions and 0, at each wavelength are shown in Table 2. It is evident that at all wavelengths the spread in the value of %D

increases with increasing angle of incidence and is more pronounced at shorter wavelengths. The ± O.s % criterion for panel spatial uniformity is clearly not satisfied in any of the three regions. Indeed, taking the panel as a whole, ± 2% is more typical.

There are several possible explanations for the evidence of the slight divergence in the data at large view angles. The incident power onto the panel is constant throughout each run. Therefore with increasing θ_r, the signal level on the detector viewing the light scattered from the panel is reduced, Since the noise level is constant, there is a reduction in experimental precision with increasing θ_r. Since the value of %D in this region is calculated from differencing two smaller numbers, then it will contain an increased percentage error with increasing view angle. 'l'he reflection of light from the Spectralon surface involves contributions from surface and volume scattering and the increasing range of %D with angle of incidence indicates a measurable surface effect, because surface scattering makes a relatively greater contribution to the total at large angles[5,6].

It is known that a final preparation stage of the Spectralon panel is a surface abrasion to achieve a prescribed thickness dimension and flatness specification. This is done using a seven-inch diameter disc sander with a three-inch diameter central hole to collect the debris. The final pass is always along the panel in one direction possibly leaving a helicoid pattern on the surface. It is probable that this finishing stage is the origin of the regional variation in BRF discussed above. The different tangents to the helicoid pattern across the surface -as depicted in Figure 7 - will result in the presentation of a different surface figure to the incident beam. Further, any problems in maintaining the sander face parallel to the direction of travel over the SpectraIon panel may cause non-planar

figuring of the panel face which would add to this effect. The observed wavelength sensitivity is conceivably an indicator of the physical size of the surface imperfection and it is possible to speculate that the greater spread in BRF at shorter wavelengths is a function of the depth of cut or disk grit size, where surface roughness of< 0.4 microns could lead to the accentuated effect at 442 nm.

5. Spectralon BRF: Cleat Effect

Since the cleats at the ends of the panels are not located under any of the test positions, the cleat effect would be detected only by variations in the data at position 6. Since the reflectance from Spectralon is known to be primarily volumetric in origin, it was necessary to determine if the cleats influenced the I] RF. The data above is used to probe the "cleat effect," and would be taken to be an observed trend in the data which distorts the BRF such that the value of %D>± 0.5% or, equally, any observed change in the BRF 'the origin of which can be uniquely associated with position 6 data.

It is clear from Figure 8 that the data obtained from positions 5, 6 and 7 at 442 nrn (and also observed at 632 and 859.9 nm) exhibit common variation with reflected angle and the departure from the panel average BRF shows no distinct characteristics from position 6. With only a few exceptions are there any data points with deviation outside the range O/Oil >± 0.5.

Therefore it is possible to conclude that those regions of the panel which are thicker than the norm do not cause a significant change in the BRF over the range of angles applicable to MISR

calibration, i.e. there is no observable cleat effect. The absence of a cleat effect further removes the concern that a significant fraction of the incident light is transmitted through the Spectralon and reflected from the back panel of the aluminum tray.

Figures 9,10 and 11 illustrate the panel BRF as a function of θ_r measured at positions 5,6 and 7 at all three wavelengths and for $\theta_i = 30°$, 45 and 600. The departure from Lambertian reflectance, manifest as the off-specular peak, is evident in all traces together with an observed increase in size of the off-specular peak with increasing O,. A relatively small number of aligned flat patches along the surface could act as glints for specular reflection at large angles of incidence and reflection when illuminated by the beam. This surface scattering effect is also the source of the off-specular peak. This characteristic has been observed in various materials, particularly metallic surfaces, and has been identified as a consequence of the dominance of the surface component of the material reflectance over that of the bulk material at large incidence and reflected angles.[7]

It is also apparent that there is a common cross-over point at 35<0, < 40°. The measured BRF in this region is constant to within 0.4% and independent of angle of incidence for 30°<6, < 60° and wavelength. Deployment of the goniometer-mounted calibration photodiode on MISR at this particular angle of reflection may therefore provide a constant reference point for in-flight calibration and establishment of a radiometric scale when the solar angle lies between 30°<0, < 60°.

6. Spectralon Reflectance Isotropy

Characterization of the isotropy characteristic of the EM panel follows from a correlation (to within ± O. 10/0) between the panel reflectance data obtained with the panel positioned with the normal at plus and minus angles relative to the wavevector of the incident beam, corresponding to $\phi_i = 00$ and 180°. Accordingly, the isotropic nature of the panel reflectance was measured at 0,= 450 and for $-70 < \theta_r < 70°$ where $\theta_r = 00$ corresponds to the detector at the panel normal. The panel was tilted ± 30° relative to the principal plane and one run was also taken in the principal plane. The data sets obtained from the plus and minus incidence angles are compared as their difference divided by their average as Ratio Difference % (not %D). The comparison for the three tilt angles shows the panel anisotropy as presented in Figure 12.

As a further control experiment to test the influence of different surface preparation on the isotropy characteristic of the panel material, a test piece of pressed polytetrafluoroethy lene (PTFE) powder was made. This 3 inch diameter panel had no machined surface finish and was tested similarity for isotropy. It is evident from Figure 13 that the ± 10/0 anisotropy measured in this case is a significant improvement over that of the EM panel and corroborates the "hypothesis that surface treatment is the source of the regional BRF and the reflectance anisotropy.

In a final stage of Spectralon characterization, two MISR protoflight panels were subject to a less exhaustive version of the uniformity examination carried out on the EM panel. The angular range of the tests were restricted; and the data were taken from three equally spaced regions vertically across the middle of the panel representative of each of the three regions identified with the EM

panel. As a further restriction, this was done at 442 nm only since at this wavelength the trends and range of BRF were most pronounced.

The uniformity analysis was performed by comparing the ratio difference %D; and the results of which are shown in Figures 14 and 15 for each of the two protoflight panels. It is clear that the proto-panels have a much more uniform surface than the EM panel and indeed satisfy the ± 0.5% range in %D established as the uniformity criterion. When the BRF measurements at positions 5,6,7 for the protoflight panels were contrasted at the incident angles 30,45,60 degrees, the off-specular peaking remained in evidence as did the constant cross-over at 37°. These results show that the surface finish was more uniform over the protoflight panels when compared with the EM panels, but had not resulted in the surface finish becoming any more Lambertian in character.

7. **Conclusions**

The optical reflectance spatial uniformity of a large Spectralon panel has been quantified by the measurement of the bidirectional reflectance factor (BRF) at eleven spatially distinct locations. Principal plane measurements at wavelengths of 442, 632 and 859.9 nm for incidence angles, θ_i, of 30 0, 450 and 60" and, for reflected angles of 0°<0,<700, reveal BRF spatial uniformity at the ± 2°A level.

Three distinct regions on the EM panel - distinguished by their distinct BRF characteristics relative to the panel average - have been identified. These are considered to be a consequence of the surface preparation of the Spectral on panel in the final stage of fabrication, substantiated by measurements

of a pressed polytetrafluoroethylene (PTFE) powder target in which no such variation was observed. This regional spread in the measured BRF is observed to be wavelength dependent and to increase with angle of incidence.

The BRF plots reveal a cross-over region for 35<0,<40°. The measured BRF in this region is constant to within 0.4°/0 and independent of angle of incidence for $300 < \theta_i < 60°$ and for three wavelengths. Therefore, since the panel reflectance is constant in three wavelength bands and independent of solar angle between 300<0, $< 60°$, this may therefore provide a valuable reference point for in-flight calibration and the establishment ofa radiometric scale.

A deviation from Lambertian reflectance, manifest as an off-specular peak in the forward scattering direction, is also observed in all three wavelength bands. This is due to the relatively larger influence of the surface reflectance component compared with volume scattering at large angles.

Similar measurements and analysis of two protoflight SpectraIon panels reveals panel uniformity at the ± 10/0 level, representing a significant improvement in surface finish and closer to the uniformity criterion of ± O. S"/o. However, no appreciable change was found in the off specular peaking nor in the cross-over angle. These results show an improvement in the uniformity of surface finish, but no loss in the specular characteristic of the reflectance at large angles of incidence and reflectance..

Experiments are in progress to explore the polarization dependence of the SpectraIon BRF as well

as obtaining an independent measurement of the directional hemispherical reflectance at each of the three spectral bands.

Acknowledgments:

This work was carried out at the Jet Propulsion Laboratory, California Institute of Technology, under contract with the National Aeronautics and Space. Administration (NASA). D.A. Haner is a member of the Chemistry Department, California State Polytechnic University, Pomona CA. The authors would like to acknowledge the technical support of S. Dermenjian, C. Esproles and A. Brothers and also technical discussion with C.J. Bruegge and V. Duval

References

(1) D.J. Diner, C.J. Bruegge, T. Deslis, V.G. Ford, L.E. Hovland, D.J. Preston, M.J. Shterenberg, E.B. Villegas and M. I,. White, "Development Status of the EOS Multi-angle Imaging SpectroRadiometer (MISR)," in SPIE (conference on Sensor Systems for Early Earth Observing System Platforms, Paper No. 1939-10, April 1993, Orlando FL.

(2) C.J. Bruegge, V.G. Duval, N. I.. Chrien and D.J. Diner, "Calibration Plans for the Multi-angle Imaging SpectroRadiometer (MISR)," Metrologia, 30, 213-221 (1 993)

(3) F.E. Nicodemus, J.C. Richmond and J.J. Hsia, "Geometrical Considerations and

Nomenclature for Reflectance," National Beaurea of Standards Monograph 160, National Beaurea of Standards, US Department of Commerce (1977)

(4) B.T. McGuckin, D.A. Haner, R.T. Menzies, C. Esproles, and A.M. Brothers, "Directional Reflectance Characterization Facility and Measurement Methodology," Submitted to Applied Optics

(5) K.E. Torrance and E.M. Sparrow, "Polarization, Directional Distribution and Off-Specular phenomena in Light Reflected from Roughened Surfaces" J. Opt. Sot. Am., 56, 916-925 (1966)

(6) K.E. Torrance, "Theoretical Polarization of Off-Specular Reflection Peaks," J. Heat Transfer, 91, 287-290 (1 969)

(7) D.A. Haner and R.T. Menzies "Reflectance (characteristics of Reference Materials used in Lidar Hard Target Calibration," Appl. Opt. 28, 857-864 (1989)

name of this file is 94f29100.909
JPL CALIBRATION FACILITY Wed Jun 29 10:09:09 1994
#
Operator: B: EM;BRF Test; pos'n 5; p-pol; tgt orig; det.=orig.;
Material: SpectraIon
Wavelength: 632.8nm
#
target elevation 0.000
target azimuth 30.000
sampling interval (ins) = 10.000
number of samples/position . 1000

det position	than 0 out (v)	std dev (V)	than 1 out (v)	std dev (V)	R (θ_r)	σ
0.000	3.13068	0.02068	3.00860	0.02195	1.04058	0.00175
5.000	3.11847	0.01895	3.00687	0.02041	1.03″712	0.00178
10.000	3.07094	0.01706	2.99944	0.01815	1.02384	0.00167
15.000	3.01845	0.01642	3.00772.	0.01843	1.00357	0.00174
20.000	2.91813	0.01883	3.00096	0.02103	0.9″)240	0.00160
25.000	2.81503	0.01520	2.99666	0.01767	0.93939	0.00158
30.000	2,67795	0.01437	3.00408	0.01704	0.89144	0.00156
35.000	2.54219	0.01428	3.00332	0.01838	0.84646	0.00150
40.000	2.37299	0.01448	3.01416	0.02053	0.78729	0.00142
45.000	2.18390	0.01256	3.00718	0.01824	0,72623	0.00125
50.000	1.98235	0.01085	3.01205	0.01785	0.65814	0.00119
55.000	1.75800	0.00995	3.00347	0.01796	0.58532	0.00112
60.000	1.52379	0.00810	3.01095	0.01740	0.50609	0.00106
65.000	1.27693	0.00833	3.00262	0.02008	0.42528	0.00092
70.000	1.03168	0.00649	3.00186	0.('1985	0.34368	0.00076

Table 1.

Archive data file for BRF measurement.

	Wavelength		
θ_i	442 nm	632.8 nm	859.9 nm"
30°	-2.0, +1.8	-1.2, +1.4	-1.6, +1.6
45°	-2.3, +2.1	-1.3, +1.8	-1.5, +1.5
60°	-3.0, +2.6	-1.7, +2.5	-2.3, +2.1

* using non-ratioed data

Table 2.

Percentage variation in panel BRF for 11 positions corresponding figures 4, 5 and 6 at each incident wavelength.

Figure Captions

Figure 1. Optical layout used during the study of the Spectralon reflectance properties. The laser-based system can delivered a user-defined beam of chosen size, polarization and one of three wavelengths on to the Spectralon panel. The panel is held in the 3-axis computer controlled target assembly which facilitates 360 degree rotation of the target and detector with ±30° tilt of the surface normal in and out of the principal plane.

Figure 2. Detail of the optical layout used in the measurement of Spectralon panel bidirectional reflectance function with the specific objective of characterizing panel uniformity.

Figure 3. Diagram of the Spectralon EM Panel showing the array of 11 points for which the BRF is recorded with the objective of characterizing the panel uniformity in each of the three spectral bands. Dimensions are in millimeters

Figure 4. The regional variation in SpectraIon panel BRF as measured at 442 nm with $\theta_i = 600$ and as a function of reflected angle: the four traces following, a downward slope are from positions 1 - 4 while those rising with a positive gradient are from positions 8-11. The group of three are from positions 5, 6 and 7 located along the middle of the panel. Note that %D = O represents the panel average.

Figure 5. 'l'he variation in panel BRF with reflected angle for the panel oriented at an angle of incidence of 60° and for an incident wavelength of 632.8 nm. Again there is evidence of three distinct responses corresponding to data recorded at positions 1-4, 5-7 and 8-11. The run to run repeatability is < 0.2°/0.

Figure 6. The SpectraIon spatial uniformity as measured at 859.9 nrn. The trends previously observed at 442 and 632.8 nm indicative of a regional BRF are less pronounced at this longer wavelength. 'l'his maybe an indicator to the size of the surface effect giving rise to the regional effect or due to any effect being concealed by the absence of ratioing in the data and the resultant greater spread in the data through the loss of precision,

Figure 7. Possible scenario through which the observed "regional" variation in measured EM panel BRF may have been created. The final surface preparation stage is a sanding to remove the specular reflection from the smooth surface and to reduce the thickness to a prescribed value. The three distinct tangential velocities could be the origin of the three regions, any off-level orientation of the sander could cause figuring of the surface and the direction of the final pass could be the origin of the measured "anisotropy" in panel reflectance.

Fugure 8. Variation in the panel BRF across the three central positions (5, 6 and 7) at 442 nm with the panel oriented at 60° relative to the incident beam. The absence of a discernible variation in BRF uniquely identifiable as originating in position 6 data is ecidence that the "cleat" is not having an effect on the panel BRF. A similar response is evident at 632.8 and 859.9 nm.

Figure 9. SpectraIon BRF as a function of the view angle at wavelength of 442 nm measured from positions 5, 6 and 7 with θ_i = 30°, 450 and 60°. The traces indicate a common BRF (to within ± 0.40A) at reflected angle of -370 and an off-specular peak. Repeatability is <0.2%.

Figure 10. Spectralon BRF measured at wavelength of 632.8 nm from positions 5,6 and 7 with 0, = 30°, 45" and 60°. The traces indicate the same feature as those measured at 442 nm: a common BRF is measured at reflected angle of -370 and an off-specular peak, Repeatability is <0.2%.

Figure 11. Specralon BRF curves measured from positions 5,6 and 7 at wavelength 859.9 nm. The traces exhibit the same general features as at 442 and 632.8 nm.

Figure 12. An anisotropy in the SpectraIon panel reflectance is revealed in this plot showing the intercomparison between data files recorded with the panel oriented at θ_i = 450: ϕ_i = 0° and 1800 with an incident wavelength of 859.9 nm. Each trace corresponds to the case where the normal to the panel surface is oriented at +30° ,0° and -30° relative to the principal plane, Clearly the 0.1 % criterion for panel isotropy is not satisfied which is considered to bc further manifestation of the surface preparation.

Figure 13. Isotropic analysis of the "pressed" PTFE panel. Each trace represents the intercomparison of data obtained at θ_i = 450 :$, = 0° and 180° for the instances of the panel surface normal being at +30° , 00 and -30° relative to the principal plane. Evidently, the isotropy which is at the ±1% level is much improved over the measured for the Spectralon EM panel and is further evidence that the surface preparation is the origin of the regional BRF and anisotropy.

Figure 14. Uniformity analysis if protoflight panel 12699-4 meaasured at 442 nm. Data is recorded from three positions vertically across the middle of the SpectraIon panel separated by 15 mm. The panel satisfies the ±0.5% criterion for "uniformity." Repeatability is 0.2%.

Figure 15. Uniformity analysis of protoflight pane] 12669-5 when illuminated at 442 nm. Data recorded from three positions orientated vertically across the panel again satisfies the ±0.5% criterion for uniformity. Data repeatability is a the 0.2% level.

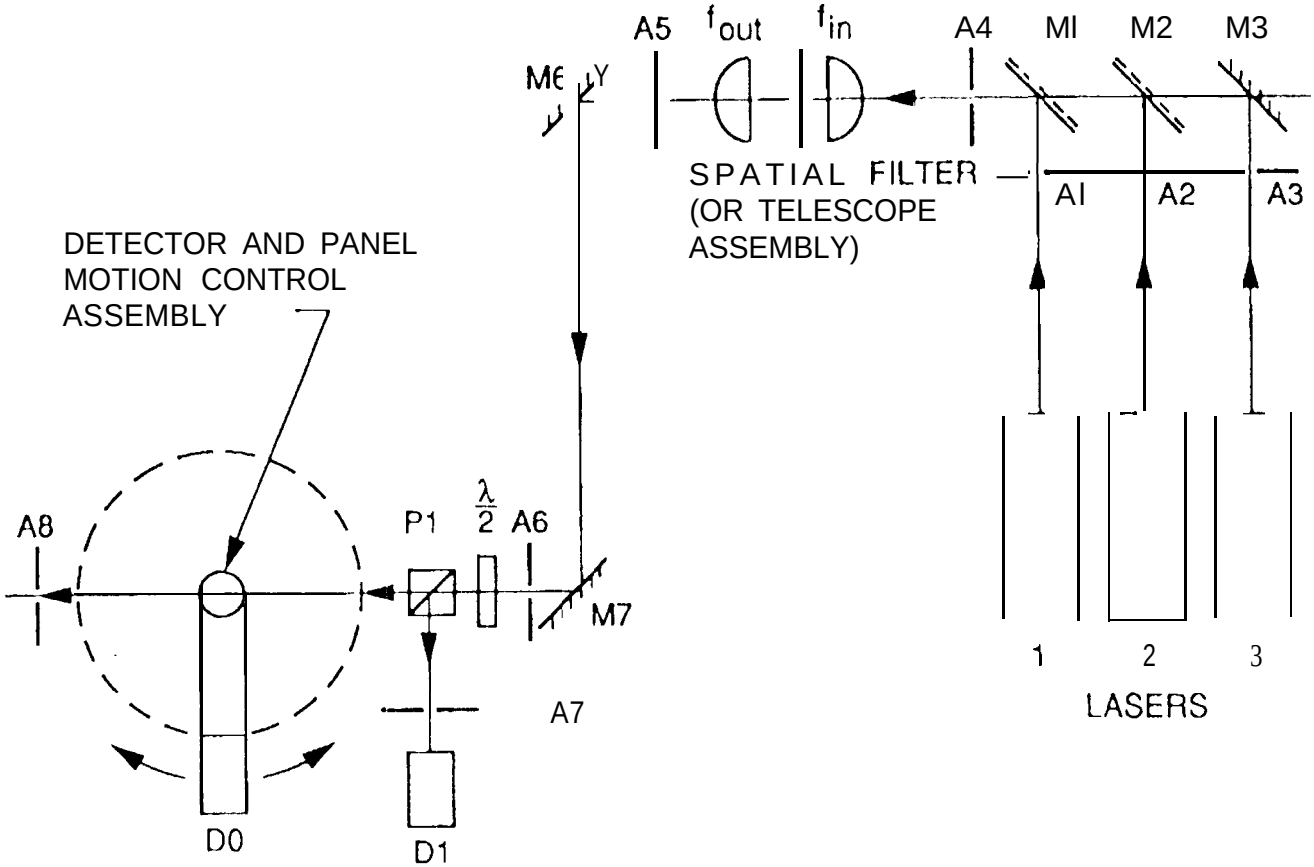
A5
f_{out}
f_{in}
A4
MI
M2
M3
M6
Y
SPATIAL FILTER
(OR TELESCOPE
ASSEMBLY)
A1
A2
A3
DETECTOR AND PANEL
MOTION CONTROL
ASSEMBLY
A8
P1
λ/2
A6
M7
A7
D0
D1
1
2
3
LASERS

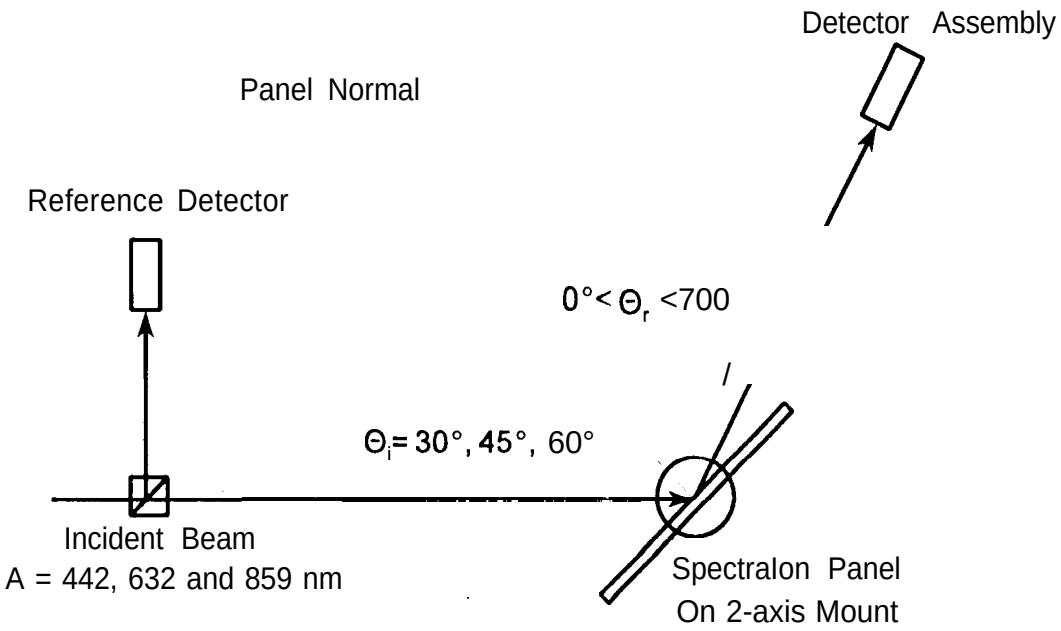
Detector Assembly
Panel Normal
Reference Detector
0°< Θr <700
Θi= 30°, 45°, 60°
Incident Beam
A = 442, 632 and 859 nm
Spectralon Panel
On 2-axis Mount

Figure 2..

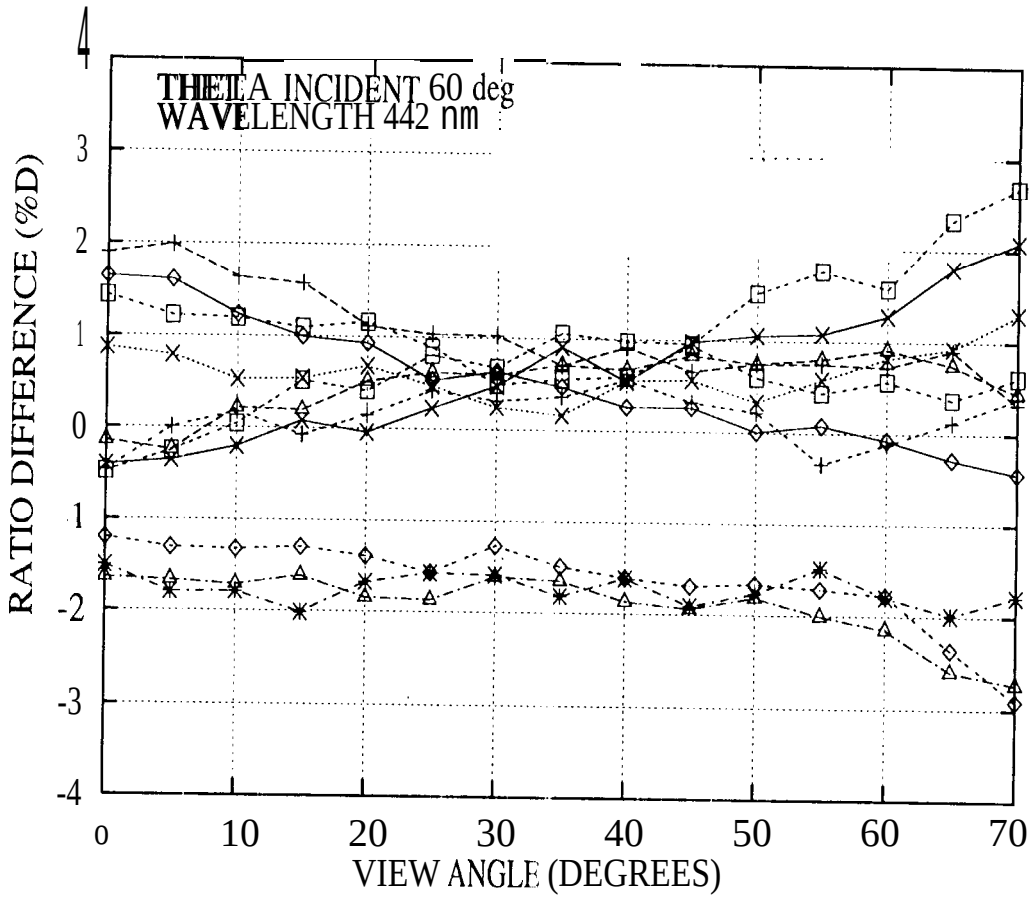
THETA INCIDENT 60 deg
WAVELENGTH 442 nm
RATIO DIFFERENCE (%D)
4
3
2
1
0
-1
-2
-3
-4
0
10
20
30
40
50
60
70
VIEW ANGLE (DEGREES)

Figure 4.

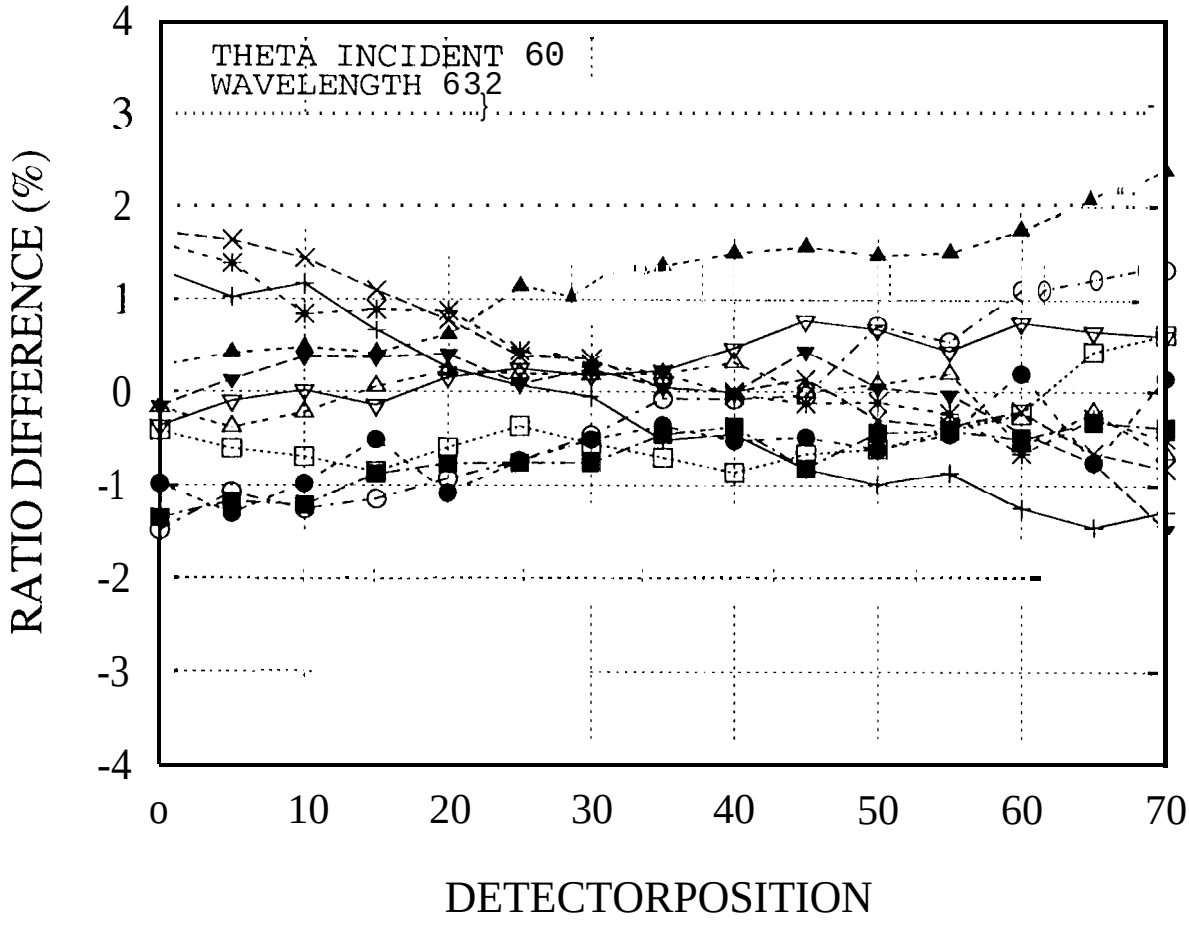
THETA INCIDENT 60
WAVELENGTH 632
RATIO DIFFERENCE (%)
4
3
2
1
0
-1
-2
-3
-4
o
10
20
30
40
50
60
70
DETECTORPOSITION

Figure 5.

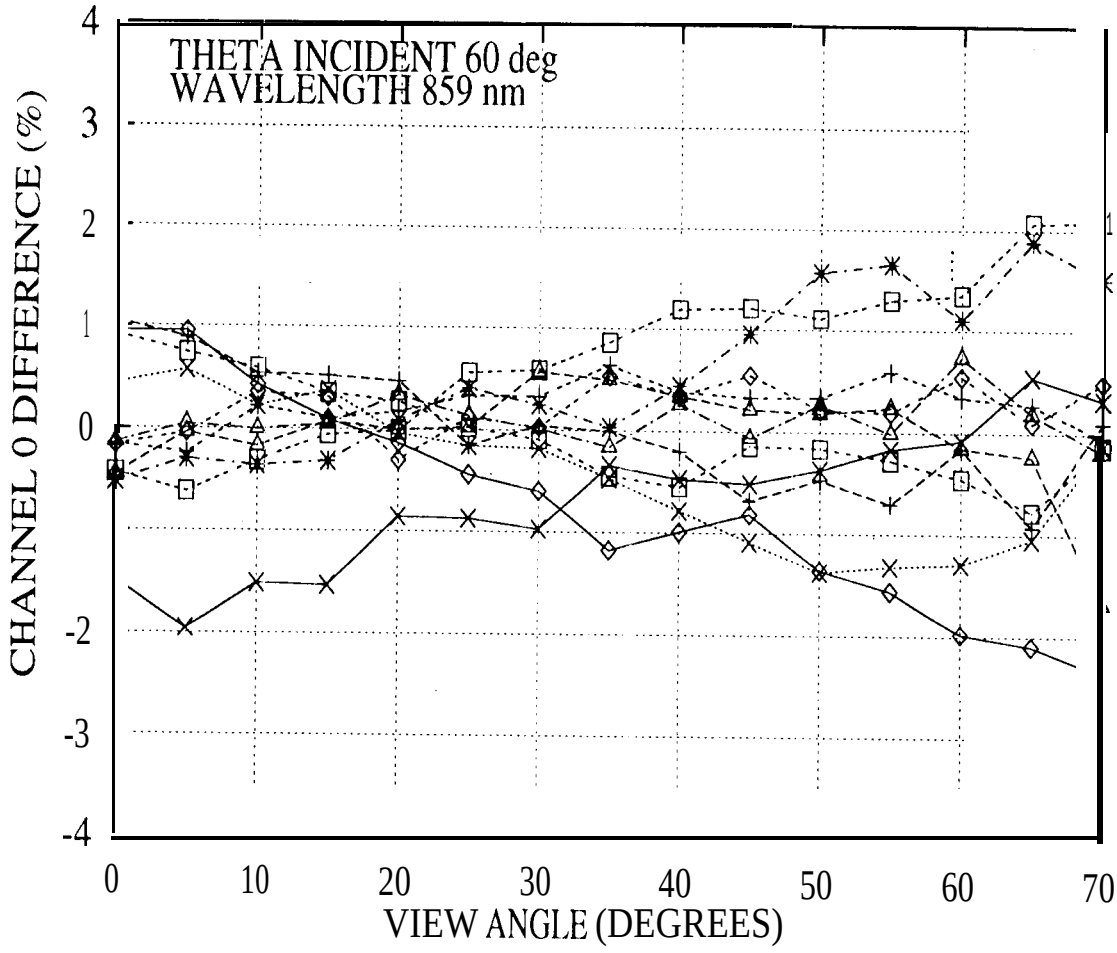
THETA INCIDENT 60 deg
WAVELENGTH 859 nm
CHANNEL 0 DIFFERENCE (%)
4
3
2
1
0
-2
-3
-4
0
10
20
30
40
50
60
70
VIEW ANGLE (DEGREES)

Figure 6.

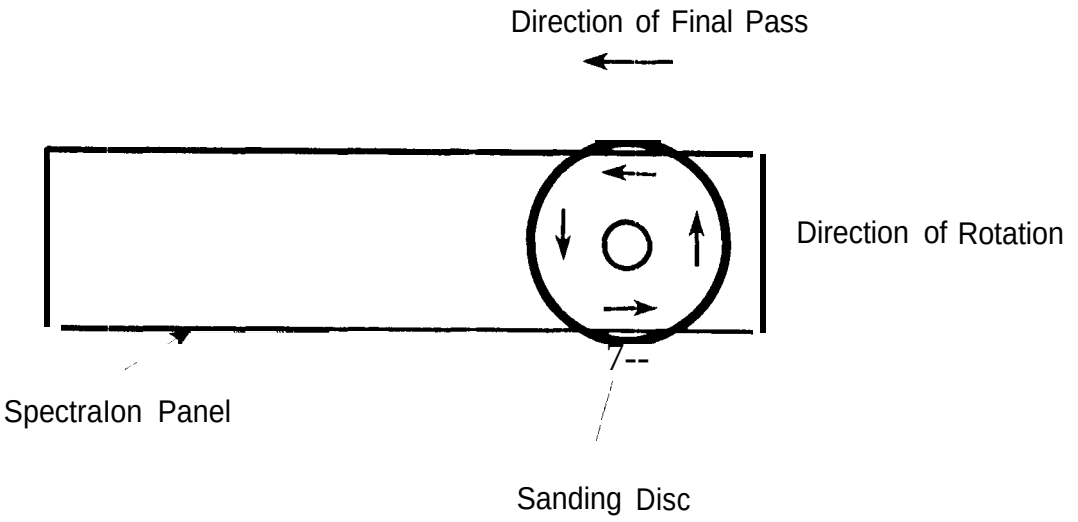
Direction of Final Pass
Direction of Rotation
Spectralon Panel
Sanding Disc

Figure 7.

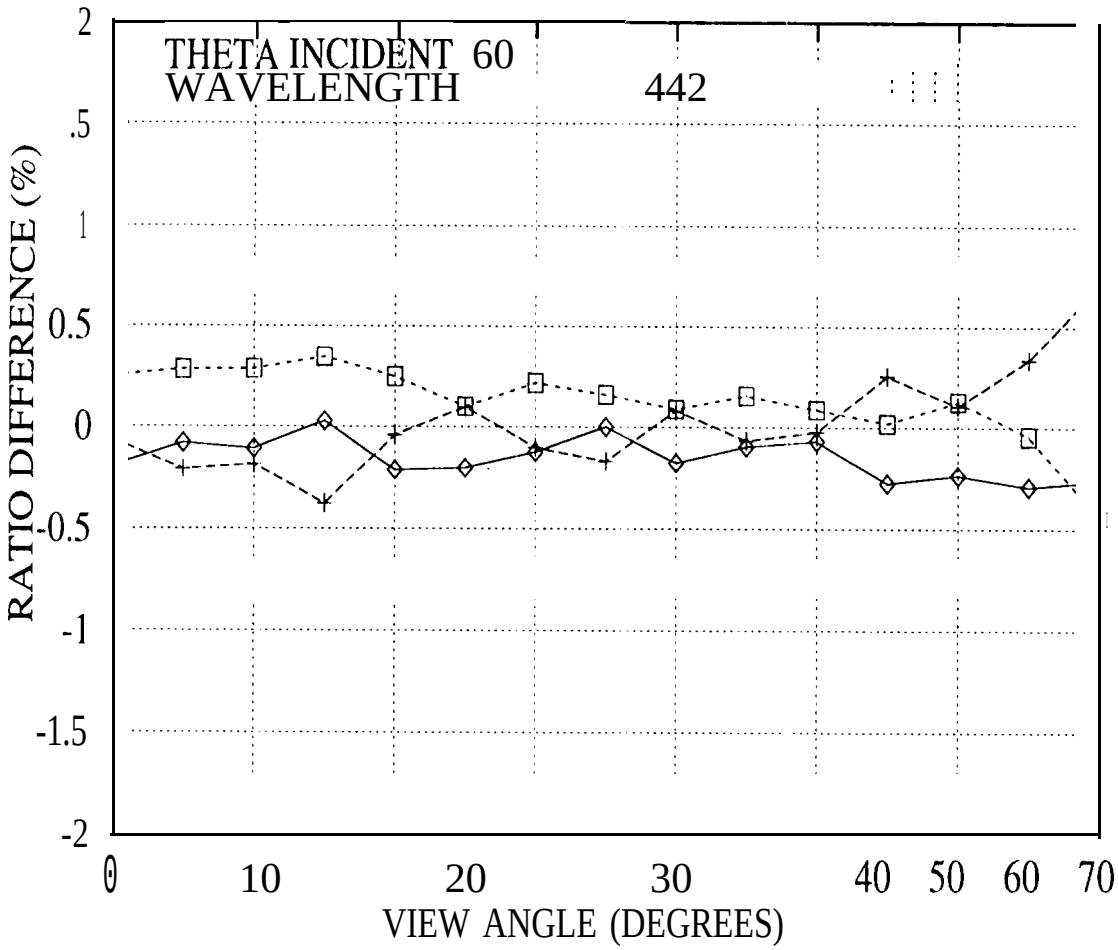
THETA INCIDENT 60
WAVELENGTH 442
RATIO DIFFERENCE (%)
2
.5
1
0.5
0
-0.5
-1
-1.5
-2
0
10
20
30
40
50
60
70
VIEW ANGLE (DEGREES)

Figure 8.

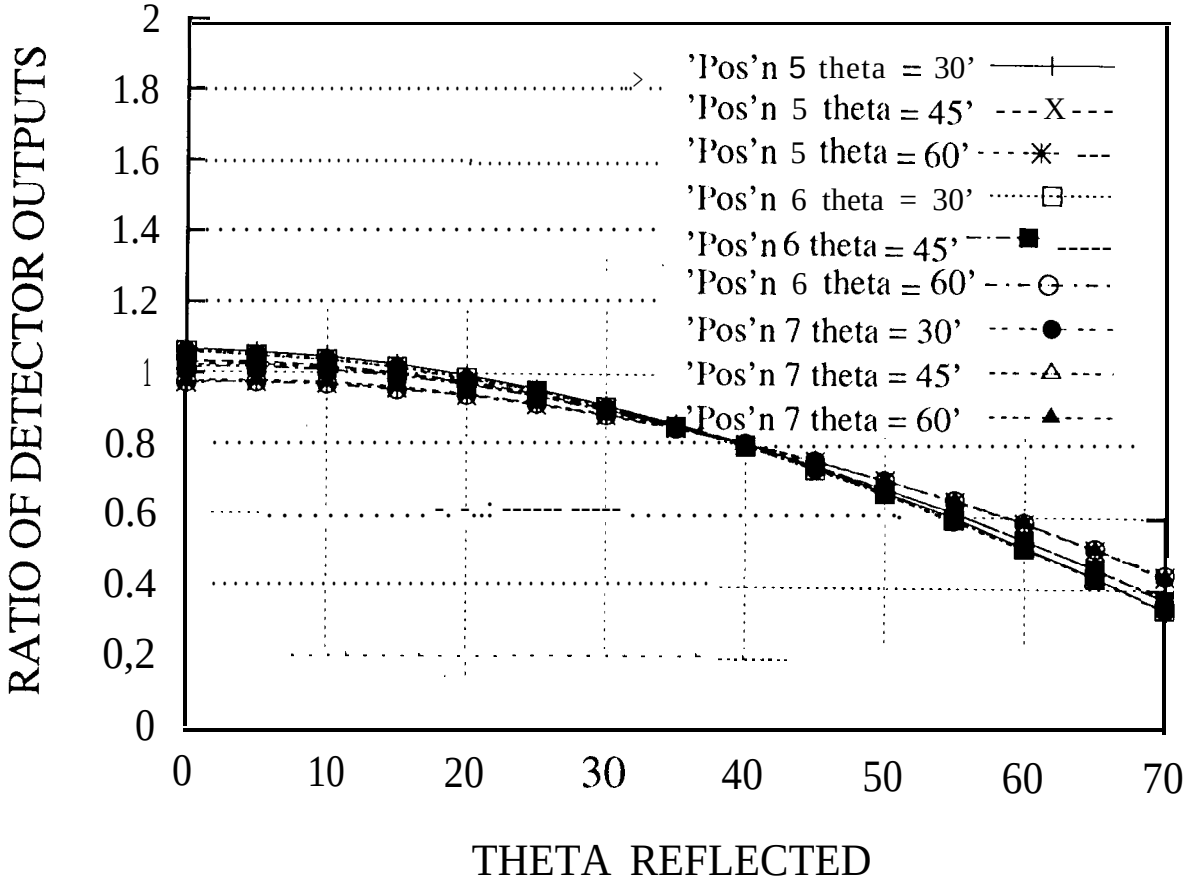
RATIO OF DETECTOR OUTPUTS
2
1.8
1.6
1.4
1.2
1
0.8
0.6
0.4
0,2
0
0
10
20
30
40
50
60
70
THETA REFLECTED
'Pos'n 5 theta = 30'
'Pos'n 5 theta = 45'
'Pos'n 5 theta = 60'
'Pos'n 6 theta = 30'
'Pos'n 6 theta = 45'
'Pos'n 6 theta = 60'
'Pos'n 7 theta = 30'
'Pos'n 7 theta = 45'
'Pos'n 7 theta = 60'

Figure 9.

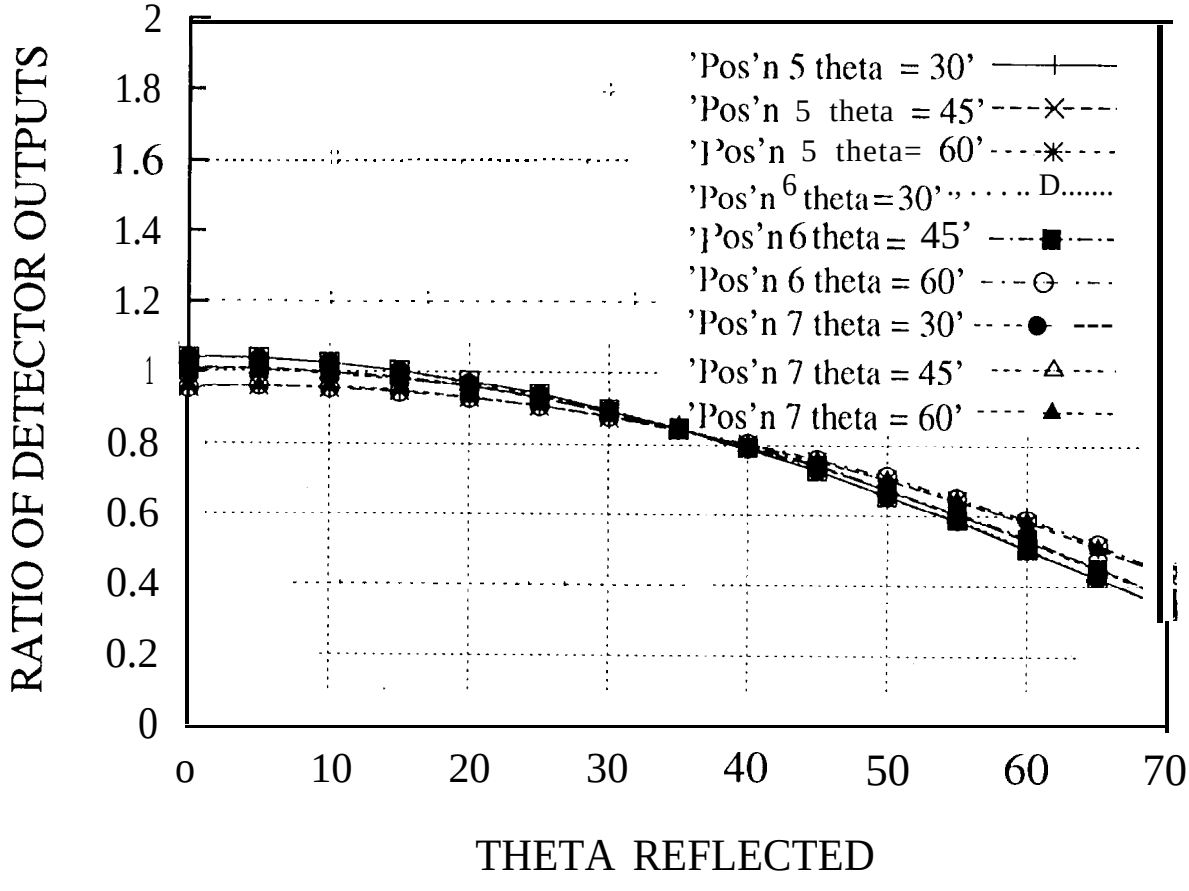
RATIO OF DETECTOR OUTPUTS
2
1.8
1.6
1.4
1.2
1
0.8
0.6
0.4
0.2
0
o
10
20
30
40
50
60
70
THETA REFLECTED
'Pos'n 5 theta = 30'
'Pos'n 5 theta = 45'
'Pos'n 5 theta= 60'
'Pos'n 6 theta=30'
'Pos'n 6 theta = 45'
'Pos'n 6 theta = 60'
'Pos'n 7 theta = 30'
'Pos'n 7 theta = 45'
'Pos'n 7 theta = 60'

Figure 10.

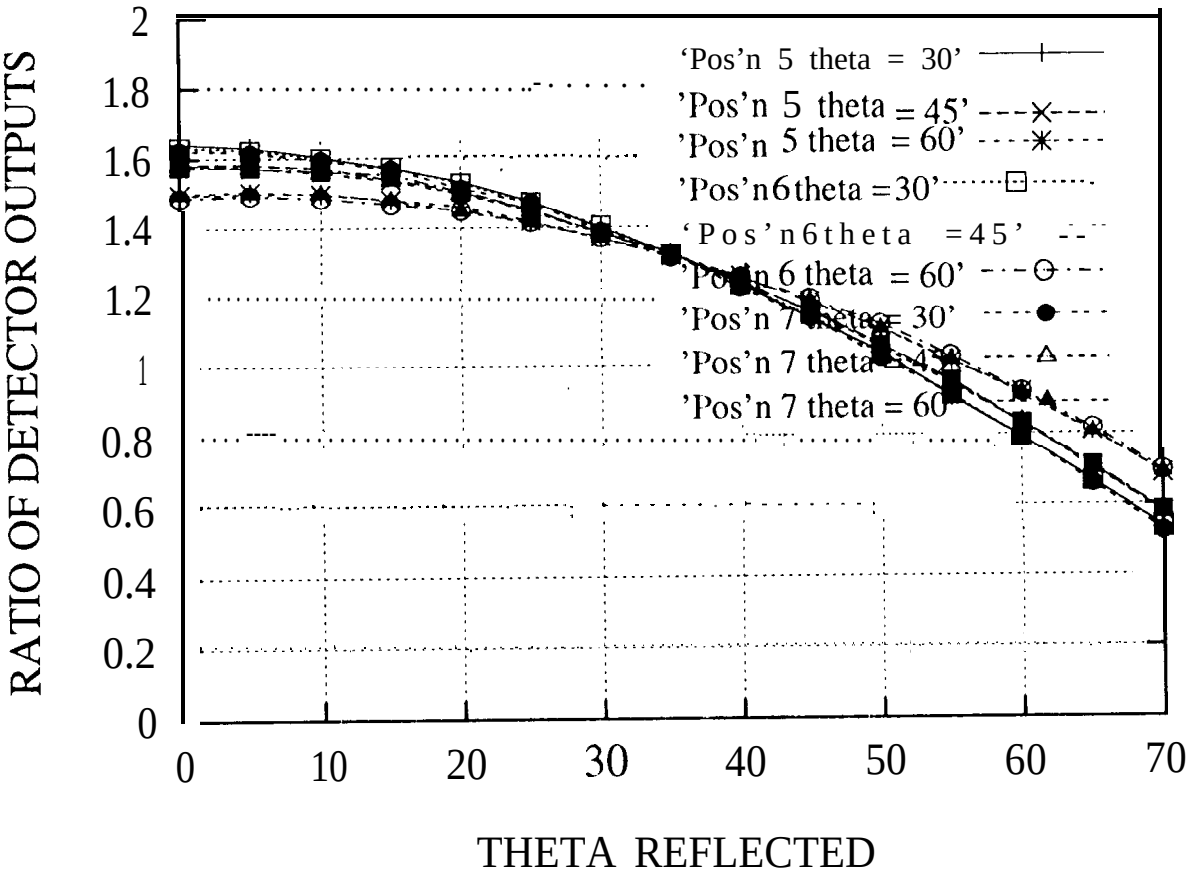
RATIO OF DETECTOR OUTPUTS
2
1.8
1.6
1.4
1.2
1
0.8
0.6
0.4
0.2
0
0
10
20
30
40
50
60
70
THETA REFLECTED
'Pos'n 5 theta = 30'
'Pos'n 5 theta = 45'
'Pos'n 5 theta = 60'
'Pos'n6theta =30'
'Pos'n6theta =45'
'Pos'n 6 theta = 60'
'Pos'n 7 theta = 30'
'Pos'n 7 theta = 45'
'Pos'n 7 theta = 60'

Figure 11.

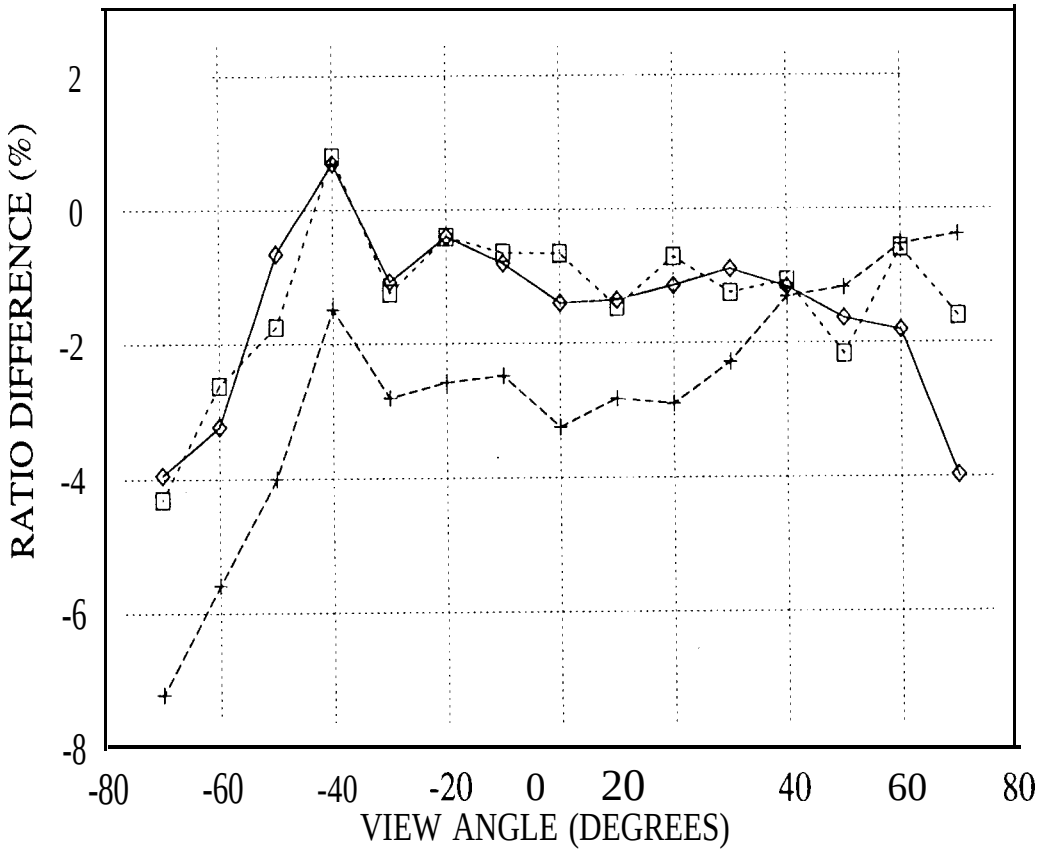
RATIO DIFFERENCE (%)
2
0
-2
-4
-6
-8
-80
-60
-40
-20
0
20
40
60
80
VIEW ANGLE (DEGREES)

Figure 12.

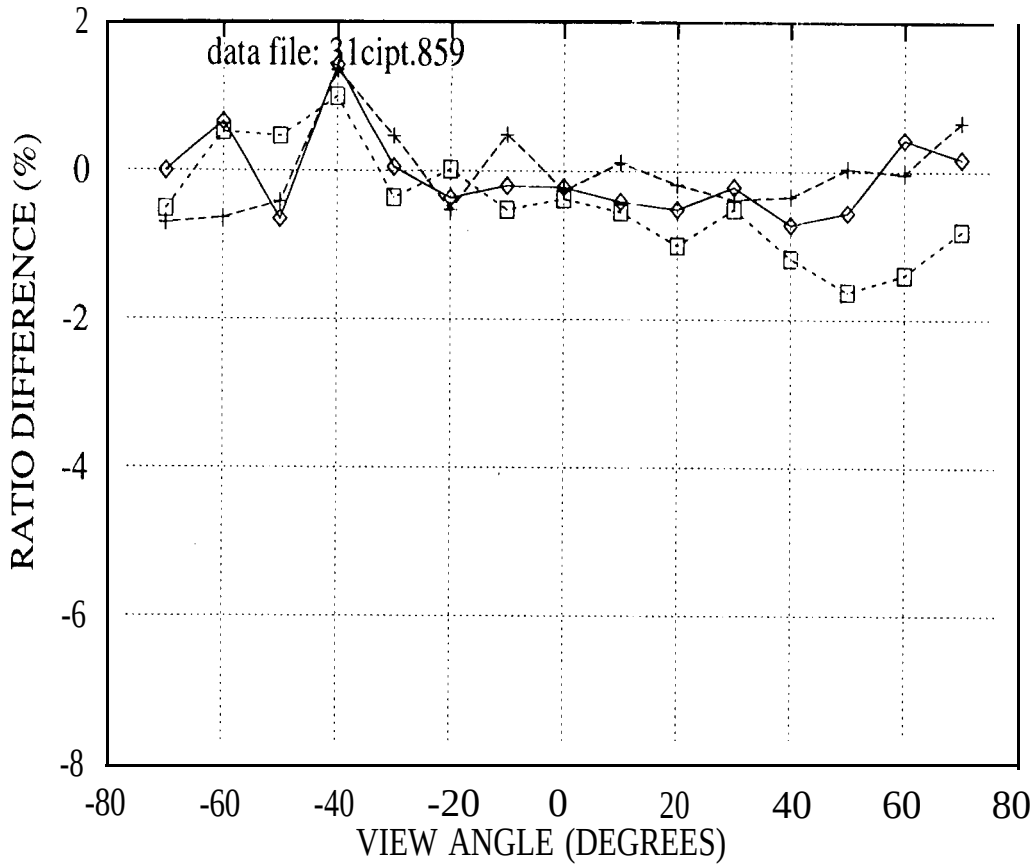
data file: 31cipt.859
RATIO DIFFERENCE (%)
2
0
-2
-4
-6
-8
-80
-60
-40
-20
0
20
40
60
80
VIEW ANGLE (DEGREES)

Figure 13.

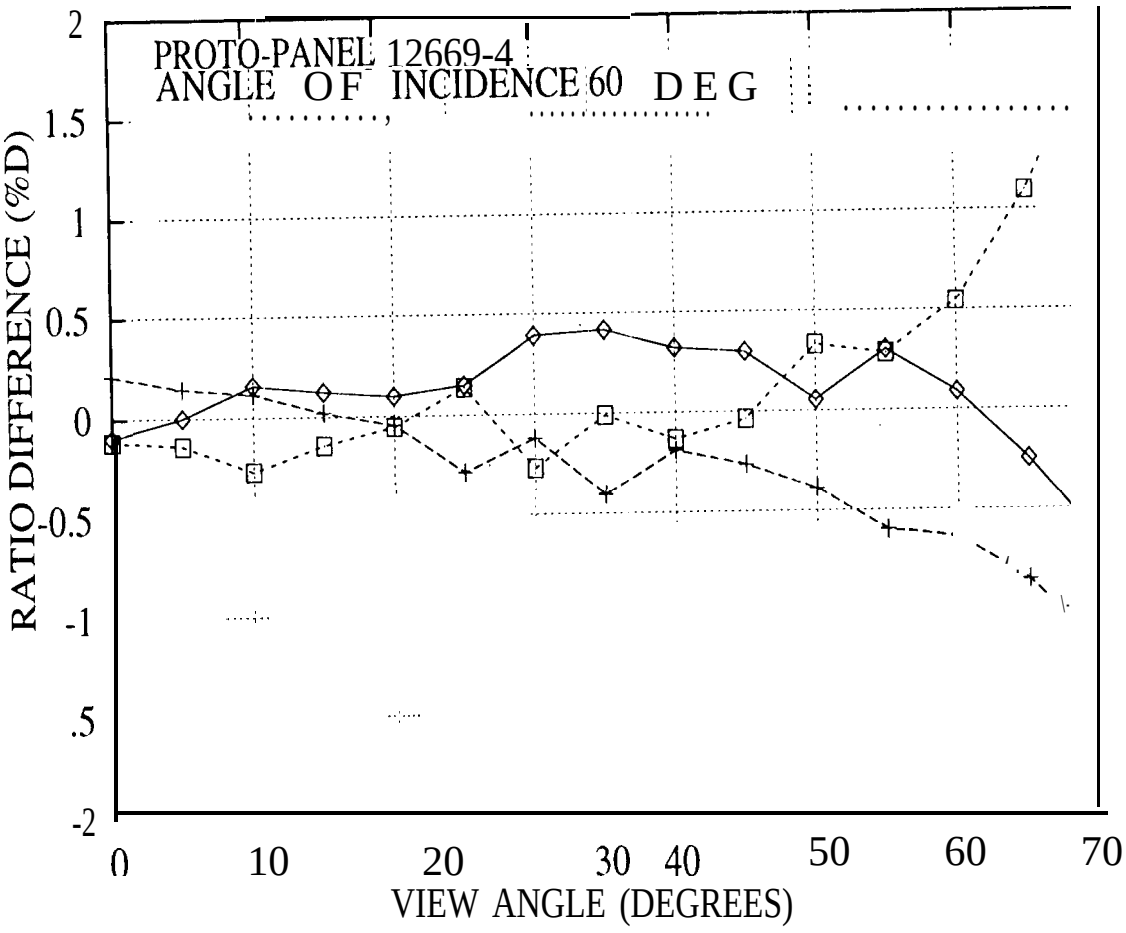
PROTO-PANEL 12669-4
ANGLE OF INCIDENCE 60 DEG
RATIO DIFFERENCE (%D)
2
1.5
1
0.5
0
-0.5
-1
.5
-2
0
10
20
30
40
50
60
70
VIEW ANGLE (DEGREES)

Figure 14.

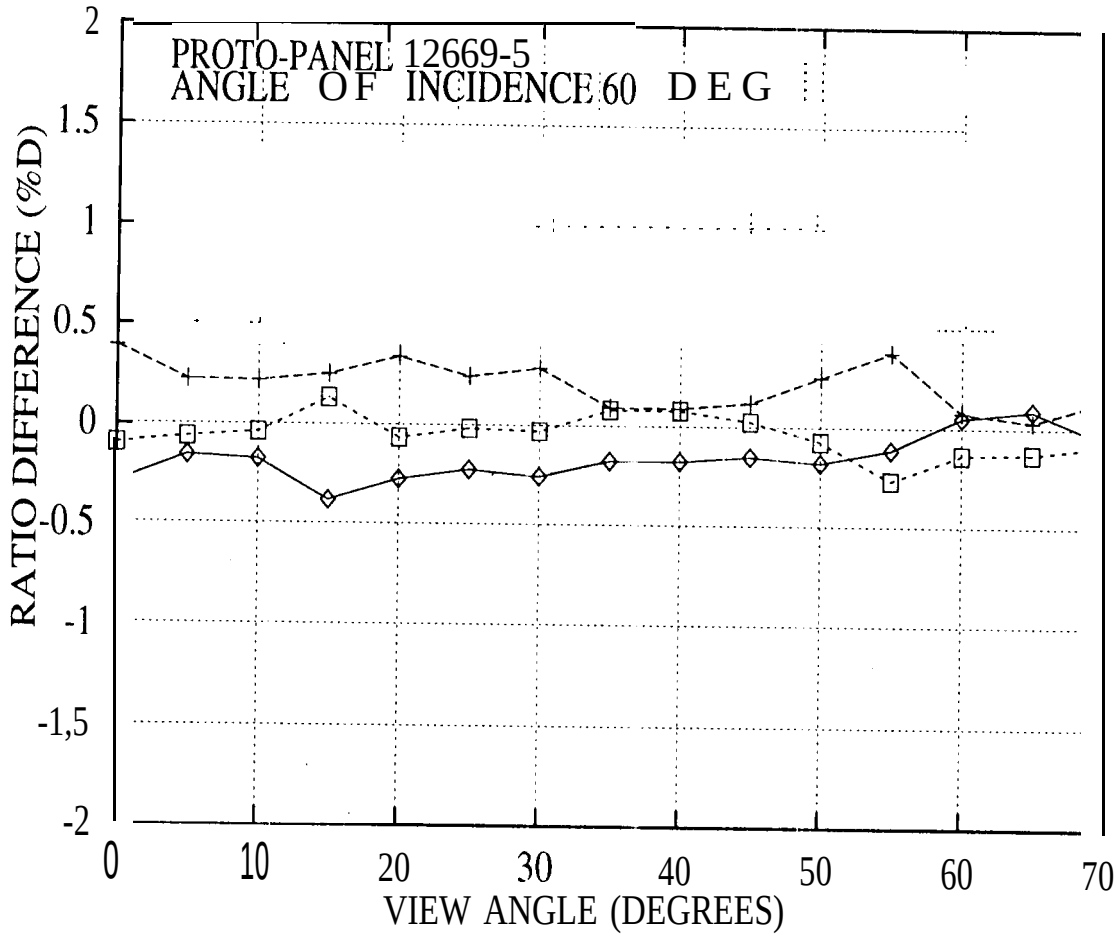
PROTO-PANEL 12669-5
ANGLE OF INCIDENCE 60 DEG
RATIO DIFFERENCE (%D)
2
1.5
1
0.5
0
-0.5
-1
-1,5
-2
0
10
20
30
40
50
60
70
VIEW ANGLE (DEGREES)

Figure 15.